3-D Terrains Deployment of Wireless Sensors Network by Utilizing Parallel Gases Brownian Motion Optimization

Min Gao[1,2], Jeng-Shyang Pan[1,2], Jian-po Li[2], Zi-pei Zhang[3], Qing-Wei Chai[1]

[1] College of Computer Science and Engineering, Shandong University of Science and Technology, China
[2] School of Computer Science, Northeast Electric Power University, China
[3] i-school Informatics, University of Washington, USA
15822553806@163.com, jengshyangpan@gmail.com, jianpoli@163.com, zzp27@uw.edu, mimanxiaowei@163.com

Abstract

With the development of Wireless Sensor Network (WSN), more and more researchers pay their attention to the deployment of sensor nodes, especially for the coverage of WSN in three dimension space. However, getting the maximum for coverage rate in WSN quickly and accurately is still a front issue. Firstly, this paper proposes a modified GBMO algorithm combining with the concept of parallel, so that the time efficiency and convergency improve to a large extend, and the search for global optimum is capable of getting faster. Then, the improvement in search and convergency efficiency of proposed PGBMO is demonstrated according to 23 benchmark functions composed of unimodal, multimodal and fixed-dimension function. Finally, a novel WSN 3-D terrain deployment scheme optimized by PGBMO is proposed to improve the coverage of the network. Experimental results demonstrate that the performance on the coverage of WSN gets efficient improvement compared to traditional particle swarm optimization (PSO) and original GBMO.

Keywords: Gases Brownian Motion Optimization, Parallel Gases Brownian Motion Optimization, Sensor Deployment, Wireless Sensor Network

1 Introduction

The searching for optimization can be explained as the process of getting some problems solved under certain conditions. The optimization can be viewed as an algorithm that dedicated to searching for optimal solutions [1-4]. Inspired by biological evolution, larger amount of optimization algorithms with different evolution strategies were presented is last decades [5-7]. Owing to that optimization algorithms imitate the habits of all kinds of creatures in nature, the optimization algorithms vary from different rules and characteristics. As a result, the problems under solved and applications for optimization algorithms are suitable for different algorithms as well. In other words, the searching for optimization is dependent on the actual functions, such as unimodal and multimodal functions. The optimization algorithm is composed of exploration and exploitation. Exploration is the process by which a group of organisms finds the best solution in situ, while the exploitation is the external search for the latest solution strategy. This paper mainly studies the evolutionary algorithm of Gases Brownian Motion Optimization (GBMO), which construct the searching for optimum based on molecular gas. Each molecule is constantly searching for the optimal solution, and finally the best solution is found through turbulent rotational motion and gases brownian motion.

At present, the WSN has been found to be very suitable in many application fields including environmental monitoring, industrial control, information security, 5G networks and disaster early warning [8-12], and the coverage rate of sensors is the main concerns. Because the current WSN implement network awareness by spreading on the network for coverage, different schemes are provided according to different sensing models to improve the network coverage [13-16]. For the sake of achieving the functional requirements in the network, a large number of sensor nodes have to be deployed in the WSN which may results in redundant coverage and waste unnecessary resources [17-19]. Therefore, effective node deployment is an important issue for current WSNs and the performance of the entire network is directly affected by the coverage of the target area. The monitor by sensors for target area can be divided into static and dynamic, which means that the sensors is either static or dynamic during the monitor [20-21]. In both cases, it can be applied to two-dimensional and three-dimensional space deployment in actual scenarios. In the early stage of WSN, network coverage based on two-dimensional plane model was paid much attention. Along with people's pursuit of real life and the need of actual scenes, 3d space node deployment has been paid more and more attention to solve many practical problems in life, such as underwater dynamic monitoring and security

*Corresponding Author: Jeng-Shyang Pan; E-mail: jengshyangpan@gmail.com
DOI: 10.3966/160792642021012201002

deployment [22-24]. It is not enough to solve these problems only by using two-dimensional coverage, so the problem of coverage in three-dimensional environments has drawn more and more attention from researchers.

Therefore, the PGBMO is proposed to optimize the three-dimensional coverage problem for WSN. The other parts are arranged as follows: Firstly, the basic GBMO algorithm and WSN 3-D coverage model are described. Secondly, a new communication strategy was introduced to improve GBMO. Thirdly, PGBMO is applied to the WSN three-dimensional coverage model. In the fourth part, the performance of PGBMO is verified by 23 test functions. Detect the pros and cons of PGBMO applied to the WSN three-dimensional coverage model in the fifth part. Finally, the work of this paper is summarized.

2 Related Works

This section focuses on the traditional GBMO and basic sensing models of WSN 3-D coverage. The GBMO is a heuristic algorithm for solving optimization problems. It is introduced as follows:

2.1 Gases Brownian Motion Optimization

In 2011, M.Abdechiri et al. proposed GBMO, which is a heuristic algorithm for simulating molecular motion [25]. To obtain a globally optimal solution, GBMO concentrates on exploring the solution through the Brownian motion of gas molecules and search for the optimal solution through the turbulent rotation motion. The concept of Brownian motion of gas molecules is to simulate the randomization of particles by the form of molecules irregular movement in the environment. In the heuristic algorithm, all particles are randomly generated, which coincides with the Brownian movement. Similarly, when a gas molecule reaches a specified limit, turbulent rotational motion enters a turbulent state. The cause of turbulence is the instability of gas molecules, which is consistent with the randomness of the molecules in the algorithm. In the GBMO, when gas molecules make brownian motion to constantly find the optimal solution, gas molecules start turbulent rotation motion for global optimal search. Through brownian motion and turbulent rotational motion, the gas molecule finally obtains the optimal solution it seeks. Based on these two motions, each molecule represents a solution. Constant molecular movement is a process of mutual achievement [26]. To facilitate the description of GBMO, it is effectively described with these basic parameters: molecular temperature T, changing number of molecules X, and molecular mass M. A detailed demonstration of the GBMO algorithm is as follows:

Step 1: Gas molecules are randomly initialized throughout the environment.

Step 2: Because the radius of each molecule is different, the radius of each gas molecule must be randomly defined. Termed R, $R \in [0,1]$.

Step 3: Initialize molecular temperature T. In the initial brownian motion, the temperature was first involved in the activity of gas molecules. In the Brownian motion of life, as the temperature increases, the gas molecules move more intensely. Correspondingly, for the participation of temperature in GBMO, the effect of the temperature on the molecule's constant motion has no doubt on the convergence of the algorithm.

Step 4: By using equation (1) and equation (2), the velocity and position of the gas molecules are updated.

$$v_i^d(t+1) = v_i^d(t) + Sign(r_1) \times \sqrt{\frac{3kT(t)}{M_i(t)}} \quad \textbf{(1)}$$

$$x_i^d(t+1) = x_i^d(t) + Sign(r_1) \times v_i^d(t) \quad \textbf{(2)}$$

Where $x_i^d(t+1)$ represents the velocity of the i-th gas molecule in the d-th dimension, just as $v_i^d(t+1)$ represents the position of the i-th gas molecule in the d-th dimension. In addition, k stands for Boltzmann constant and is set to 1.38066×10^{-23}. r_1 is a random number, $r_1 \in [0,1]$. $Sign(r_1)$ is described as:

$$Sign(r_1) = \begin{cases} -1 & if(r_1 \le 0.5) \\ 1 & if(r_1 > 0.5) \end{cases} \quad \textbf{(3)}$$

Step 5: All molecules are evaluated by calculating the objective function value.

Step 6: After continually performing the Brownian motion, the appellants formally participate in the turbulent rotational motion in the following way. Set the constants a =1.5 and b =1.2 to participate in this event. The following equations are listed to update the gas molecule position.

$$\begin{aligned} x_i^d(t+1) &= x_i^d(t) + b \times Sign(r_2) \\ &\quad - (\frac{a}{2\pi}) \times \sin(2\pi x_i^d(t)) \times Sign(r_2) \end{aligned} \quad \textbf{(4)}$$

Where r_2 is a random number, $r_2 \in [0,1]$. $Sign(r_2)$ is described as:

$$Sign(r_2) = \begin{cases} -1 & if(r_2 < 0.5) \\ 1 & if(r_2 \ge 0.5) \end{cases} \quad \textbf{(5)}$$

Step 7: Use the objective function to evaluate the molecules after turbulent rotation.

Step 8: The mass M and temperature T of the gas molecules are updated with the following equation.

$$M_i(t) = \frac{fit_i(t) - worst(t)}{best(t) - worst(t)} \quad \textbf{(6)}$$

Where the $fit_i(t)$, $worst(t)$ and $best(t)$ respectively represent the molecular fitness function value, the best value, and the worst value of the i-th gas molecule at time t.

$$T = T - \left(\frac{1}{mean(fit_i(t))}\right) \quad \textbf{(7)}$$

Where $mean(fit_i(t))$ is the average value of the function values of all molecules at time t.

Step 9: If the algorithm reaches the motion termination condition, it is terminated. Otherwise, repeat steps 4-8 until the termination conditions are met.

2.2 The 3-D Network Coverage Model

In WSN, the network coverage model and node deployment greatly affect the WSN coverage problem. The points and faces in the sensor construct a geometric relationship through the perception model. This is an important criterion for measuring the quality of sensor services. The perception model of WSN usually has 0-1 model and probability model. In this paper, we will optimize the WSN network coverage through the 0-1 model. Therefore, we will introduce the 0-1 model in detail.

0-1 model: In the WSN network coverage model, this model is the most commonly used perception model. In layman's terms, 1 represents a sensor node covered an event, 0 represents no coverage. This article combines the concept of a line-of-sight (LOS) in literature [27]. That is: there is no obstacle between the two nodes to communicate. This is absolute perception. Let the coordinates of the node S in WSN be (S_x, S_y, S_z), and the position of the target node be (T_x, T_y, T_z), The sensing radius is R, and the distance between the sensor node S and the target node T is:

$$D(S,T) = \sqrt{(S_x - T_x)^2 + (S_y - T_y)^2 + (S_z - T_z)^2} \quad \textbf{(8)}$$

According to the above, the 0-1 perception model is:

$$O(S,T) = \begin{cases} 1 & (D(S,T) < R) \,\&\, if\ LOS \\ 0 & otherwise \end{cases} \quad \textbf{(9)}$$

As can be seen from the above formula, if the three dimensional area is perceived, the probability of the perception model is 1, otherwise it is 0.

3 Our Proposed PGBMO and Its Improvement on Node Coverage of WSN

In this section, we describe the PGBMO proposed in this article and the three-digit deployment problem applied to WSN. Heuristic algorithms sometimes lead to premature convergence. The weakening of population diversity is a prominent manifestation of premature convergence. Next, we will explain in detail our proposed parallel strategy.

3.1 Parallel Gases Brownian Motion Optimization

The PGBMO uses the idea of parallelism to improve the convergence and accuracy of the algorithm [28-29]. The idea of parallelism is to divide a large population into several small sub-populations to perform tasks independently. Although each subpopulation may fall into a local optimum, as long as appropriate communication strategies are added, this situation can be prevented in time. The PGBMO evenly divides the population into p groups, denoted as $G = \{G_1, G_2, ..., G_p\}$, where $p = \{1, 2, 3, ...\}$. Let t be the number of population iterations. Whenever the iteration number for the sub-populations is at $t = R$, the sub-populations communicate, where $R = \{R_1, 2R_1, 3R_1, ...\}$. This article proposes four communication strategies. We will explain one by one.

3.1.1 Communication Strategy with Displacement

When each subpopulation is in the R iteration, each group of gas molecules communicates in GBMO. The means of communication is displacement's exchange of ideas. The following will explain in detail the displacement way of thinking. Firstly, the sub-populations of each group still perform their tasks as usual. The core of their task is still to optimize according to the original rules. Then, because each sub-population after long-term optimization may cause the gas molecule to enter a locally optimal state, when $t = R$, each sub-population starts to meet. They seek optimal solutions from each subpopulation. And compare their optimal solutions again to find the best gas molecules in all populations. We call the optimal gas molecule the winner. Finally, in each subpopulation, several gas molecules are randomly selected. We call these randomly selected gas molecules sub-random molecules. The most critical step is to use the winner to replace the sub-random molecule to complete the communication.

In general, this communication is to use the best individual in all groups to replace individuals randomly selected by each subpopulation [30]. This can effectively prevent the subpopulation from falling into the local optimality prematurely. This algorithm is called PGBMO-DC (Parallel Gases Brownian Motion Optimization-Displacement Communication). Figure 1 shows the operation diagram of the PGBMO-DC algorithm.

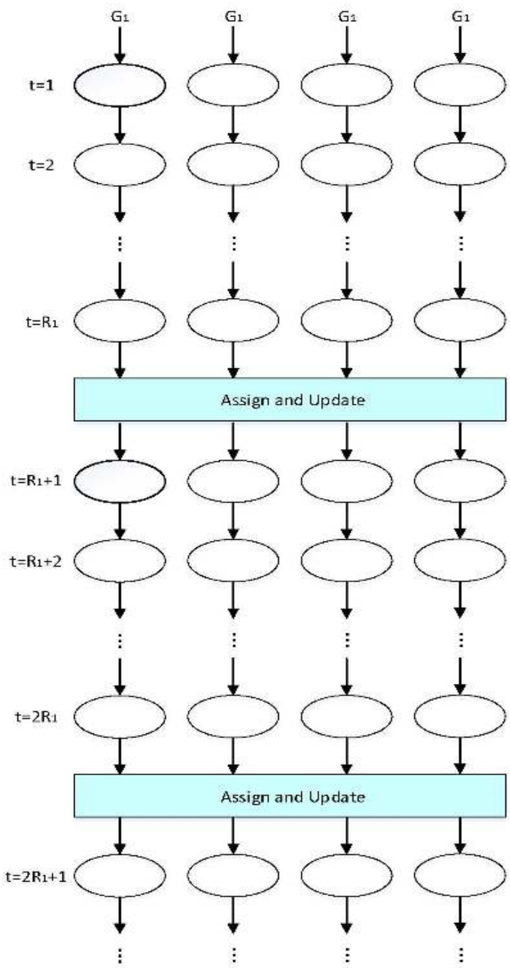

Figure 1. The PGBMO-DC Algorithm Diagram

3.1.2 Communication Strategy with Exchange Displacement

This communication chooses two different communication methods to communicate [31-32, 39-40]. When the population reaches $R=\{R_1, 3R_1, 5R_1, ...\}$, GBMO uses the idea of exchange to communicate. Exchange's way of thinking is to use the idea of survival and elimination. We will introduce specific operations in detail. Firstly, select the best gas molecule and the worst gas molecule from the sub-populations. We refer to this as a sub-winner and a sub-loser, which are denoted G_p^w and G_p^l respectively. Secondly, divide this p group into two small teams in groups of two. Suppose there are 4 groups in total, then G_1 and G_2 are a group, and G_3 and G_4 are a group. Finally, exchange operations in each small team. That is, the sub-winners in the p-th group are used to exchange with the sub-losers in the $(p+1)$-th group. And use the sub-losers of the group p to exchange with the sub-winners of the group $p+1$. Mathematically described as follows:

$$G_p^w \underrightarrow{replace} G_{p+1}^l \tag{10}$$

$$G_{p+1}^w \underrightarrow{replace} G_p^l \tag{11}$$

The local optimum can be effectively avoided by the mutual exchange of subpopulations. It is the subtlety of this algorithm to exchange the worst value of each group with the best in time. However, merely switching the optimal is not enough to make the algorithm reach a good state. Therefore, when $R=\{2R_1, 4R_1, 6R_1, ...\}$, we use the communication method of PGBMO-DC algorithm to communicate. This avoids the monotony of the algorithm. Combining the two ideas of exchange and displacement can diversify the algorithm and effectively avoid the appearance of local optimization. We call this algorithm PGBMO-EDC (Parallel Gases Brownian Motion Optimization-Exchange Displacement Communication). Figure 2 gives a detailed description of the PGBMO-EDC algorithm.

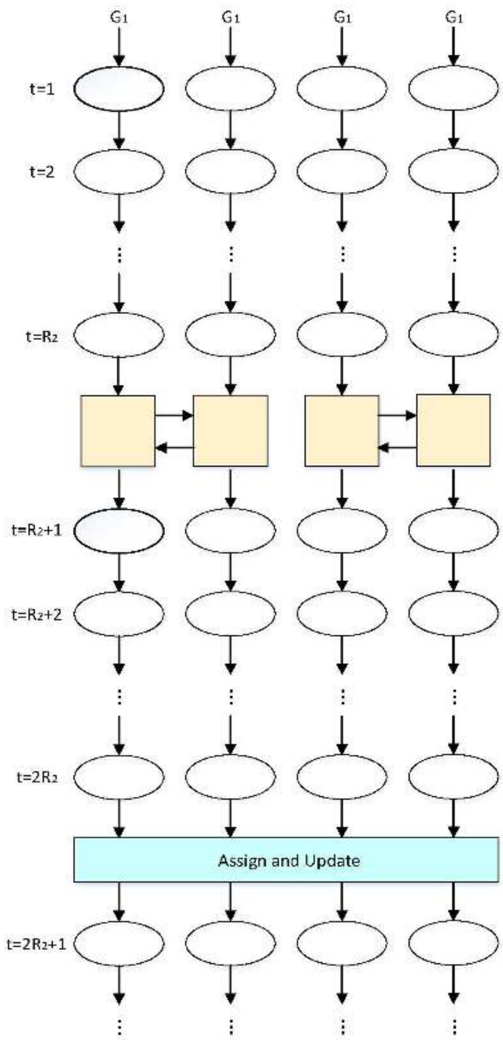

Figure 2. The PGBMO-EDC Algorithm Diagram

3.1.3 Communication Strategy with Switch Regrouping

If each subpopulation continues to seek optimization through the original orbit, then this will lead to huge differences between the subpopulations [33]. It may cause each sub-population to develop toward the optimal they think, rather than the global optimal. Therefore, the communication strategy used this time is to optimize the algorithm through the idea of communication regrouping to find the global optimal. When each subpopulation iterates to $R=\{R_1, 3R_1, 5R_1, ...\}$, each subpopulation begins to pass through. The idea adopted this time is the philosophy of Switch. After each of their sub-populations

finds sub-winners G_p^w and sub-losers G_p^l, randomly selects the x group to switch. That is, randomly select x groups in the $p(x<p)$ group to save their G_p^w. Then randomly select $y(x=y)$ group to save their G_p^l. Finally, use the G_p^w of these x groups to randomly replace G_p^l of the other y groups. They will regain their fitness function. However, only the idea of communication is not sufficient for perfect optimization, so when $R=\{2R_1, 4R_1, 6R_1, ...\}$, let each subpopulation be regrouped. Regrouping is a method of random grouping. Random grouping is equivalent to adding a good disturbance to increase the search space. This can ensure population diversity and prevent each subpopulation from falling into a local optimum.

In short, our communication method uses not only switch but also the concept of Regrouping, so we call this communication strategy PGBMO-SRC (Parallel Gases Brownian Motion Optimization-Switch Regrouping Communication). Figure 3 shows the communication strategy of PGBMO-SRC.

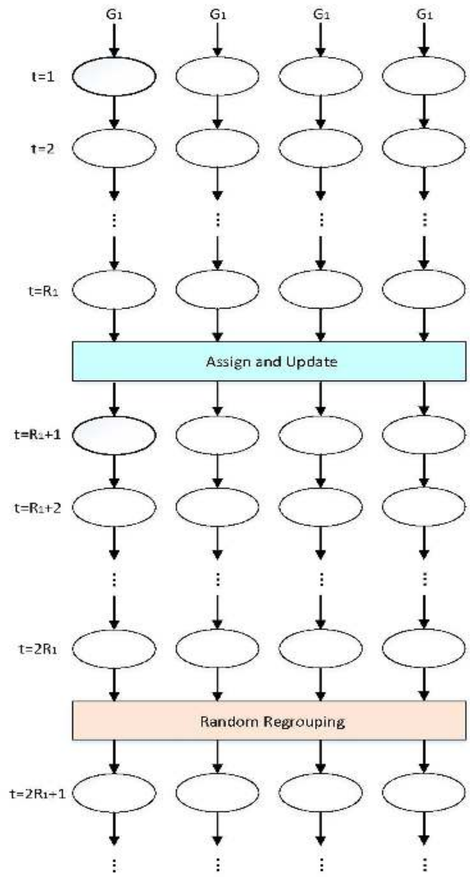

Figure 3. The PGBMO-SRC Algorithm Diagram

3.1.4 Communication Strategy with Displacement Regrouping

This article combines the displacement idea of PGBMO-DC with the idea of Regrouping in PGBMO-SRC to achieve optimization. That is, when $R=\{R_1, 3R_1, 5R_1, ...\}$, use displacement's way of thinking to communicate; when $R=\{2R_1, 4R_1, 6R_1, ...\}$, regroup the entire population randomly. We will all the communication strategy of this hybrid program PGBMO-DRC (Parallel Gases Brownian Motion Optimization-Displacement Regrouping Communication). Figure 4 shows the communication method of PGBMO-DRC.

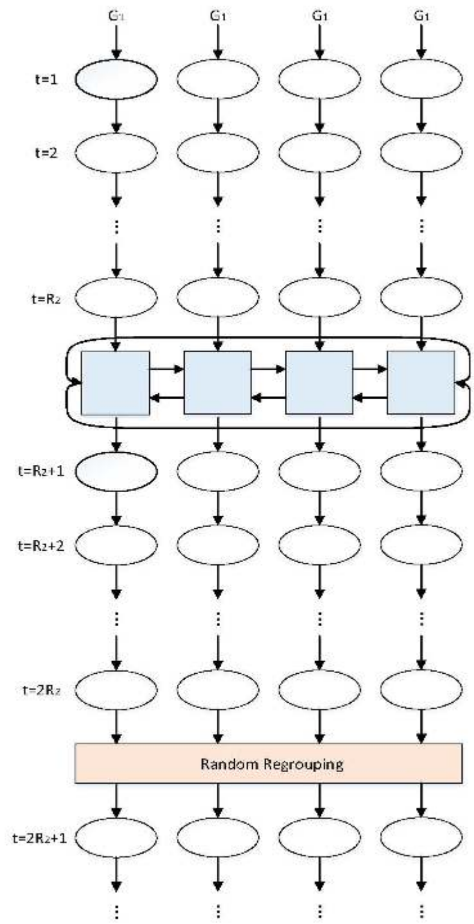

Figure 4. The PGBMO-DRC Algorithm Diagram

3.2 The PGBMO Application in WSN Based on Node Coverage

This article is aim to solve the problem of coverage the maximize area in 3-D terrain with limited number of sensor nodes. There are many ways to solve the problem of two dimensional plane coverage [34], and achieved good performance. However, the simulation of placing sensor nodes on a two dimensional plane is obviously different from the real-world problem. In order to more actually simulate the coverage problem, this paper layout the sensor nodes on 3-D terrain.

Solving the coverage problem essentially is find the optimal deployment strategy. The different strategies have a significant influence to coverage rate especially on 3-D terrain. In recent years, many researchers utilized the intelligent computing algorithm to settle similar problems [35]. This paper improves the performance of GBMO by applying communication strategy and uses this novel algorithm to solve the coverage problem of WSN on 3-D terrain.

In a specific 3-D terrain, if you know the value of any two coordinates of a point, you can calculate the value of the third coordinate of the point. Therefore, the algorithm can optimize the deployment strategy by optimizing the sensor node positions in any two dimensions. Every individual of algorithm represents a deployment strategy, so the individual is initialed as Figure 5:

$POS_{1,1}$	$POS_{2,1}$	II II	$POS_{n-1,1}$	$POS_{n,1}$
$POS_{1,2}$	$POS_{2,2}$	II II	$POS_{n-1,2}$	$POS_{n,2}$

Figure 5. Design of Individual Dimension Values

Each individual update their position according to equation (12) and evaluate their fitness according to the following equation:

$$R(i) = \frac{1}{M}\sum_{q=1}^{M}\left(\sum_{p=1}^{P} O(S_p, T_q)\right) \quad \textbf{(12)}$$

Where $R(i)$ represents the population coverage rate at the i-th iteration. P is defined as the number of sensors. M represents pixels on the 3-D terrain. $O(S_p, T_q)$ represents whether the q pixel is covered by the p sensor, and it is obtained by the equation (9).

4 Experimental Simulation and Analysis of The Proposed Algorithm

In this section, to prove whether the parallel communication strategy is effective, we used 23 test functions to test its performance. The test environment is MATLAB 2015b. Referring to the literature [36-37], The Figure 6 to Figure 8 respectively enumerate 2-D versions of unimodal, multimodal, fixed-dimension functions in order to understand the functions more clearly.

4.1 Parameter Arrangement

To verify the performance of the proposed algorithm, we compare them with PSO and GBMO. Also, keep the parameter settings of each of them consistent. They run an average of 30 tests on each test function for comparison experiments. To better comprehend the convergence of each algorithm, the number of iterations ($Iteration$) is set to 1000. For testing the performance of each parallel strategy fairly, we divide the proposed several parallel algorithms into 4 groups. That is, g = 4. And R_1 is set to 20, that is, exchange or regroup every 20 times. Table 1 lists the parameter settings of these algorithms. The specific algorithm process of the PSO algorithm refers to the literature [38]. Here we set the constant c to 2.0 and the weight w to 0.9. In GBMO and the four parallel strategies, a is set to 1.5 and b is 1.2. Their temperature T initialization is set to 900, and the Boltzmann constant k is set to 1.38066 × 10^{-23}. And the population of these several algorithms (pop) is set to 40.

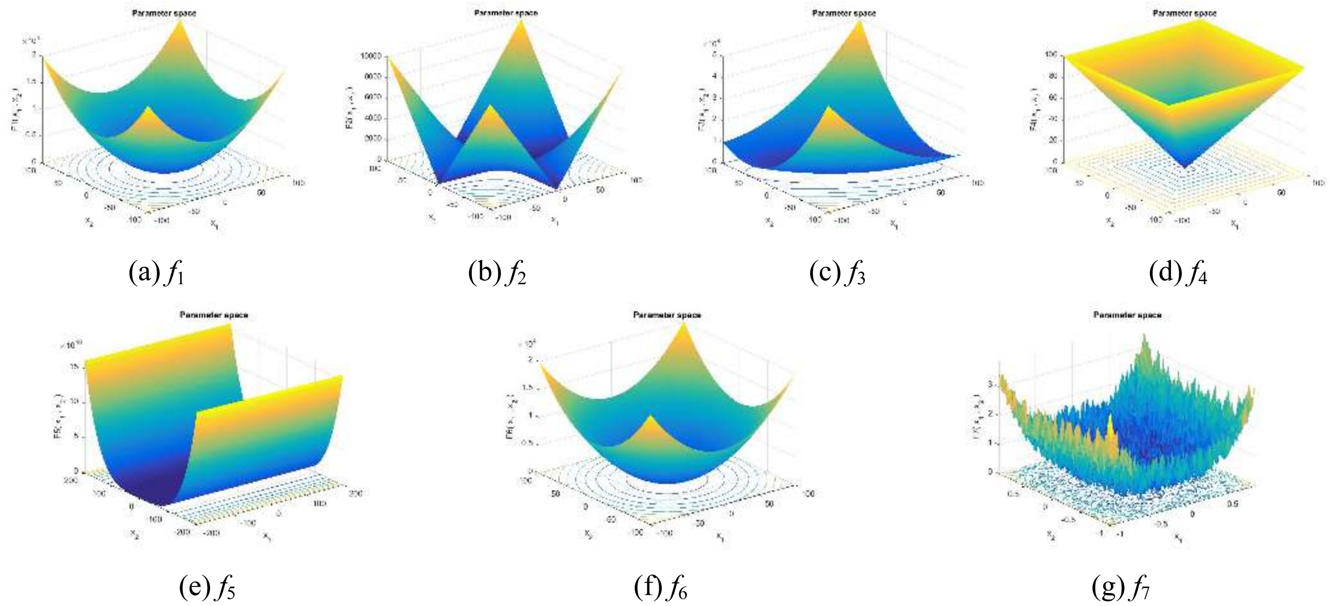

(a) f_1 (b) f_2 (c) f_3 (d) f_4

(e) f_5 (f) f_6 (g) f_7

Figure 6. 2-D Versions of Unimodal Benchmark Functions

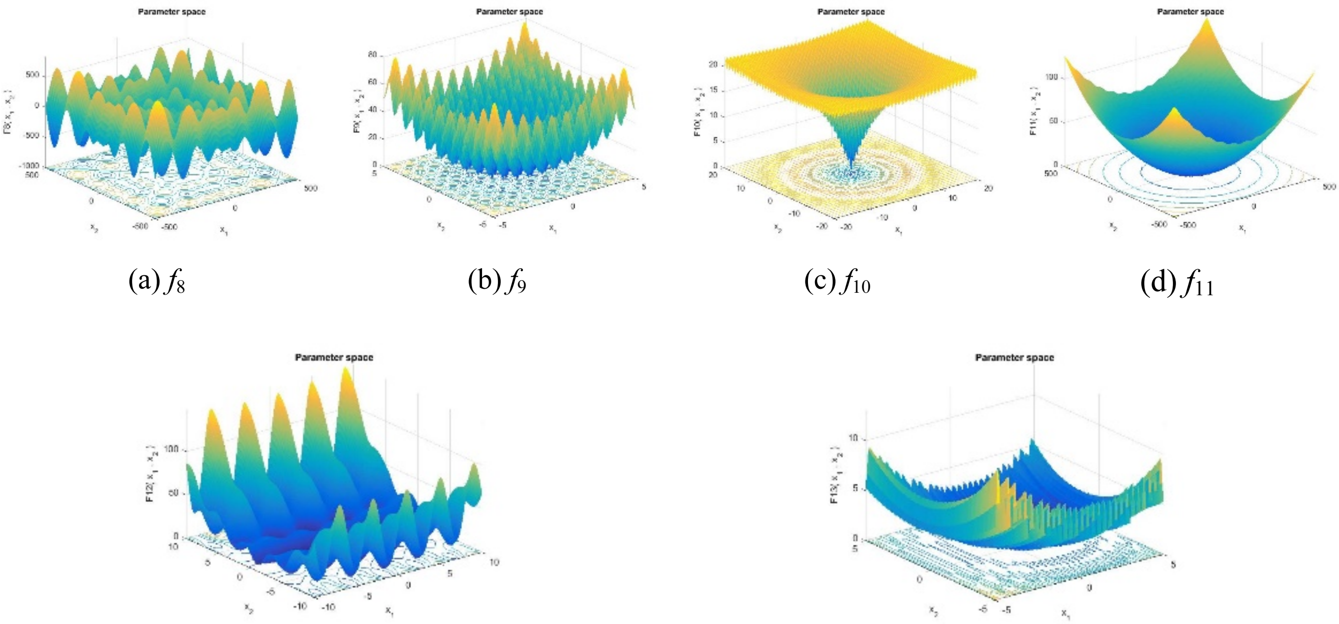

(a) f_8 (b) f_9 (c) f_{10} (d) f_{11}

(e) f_{12} (f) f_{13}

Figure 7. 2-D Versions of Multimodal Benchmark Functions

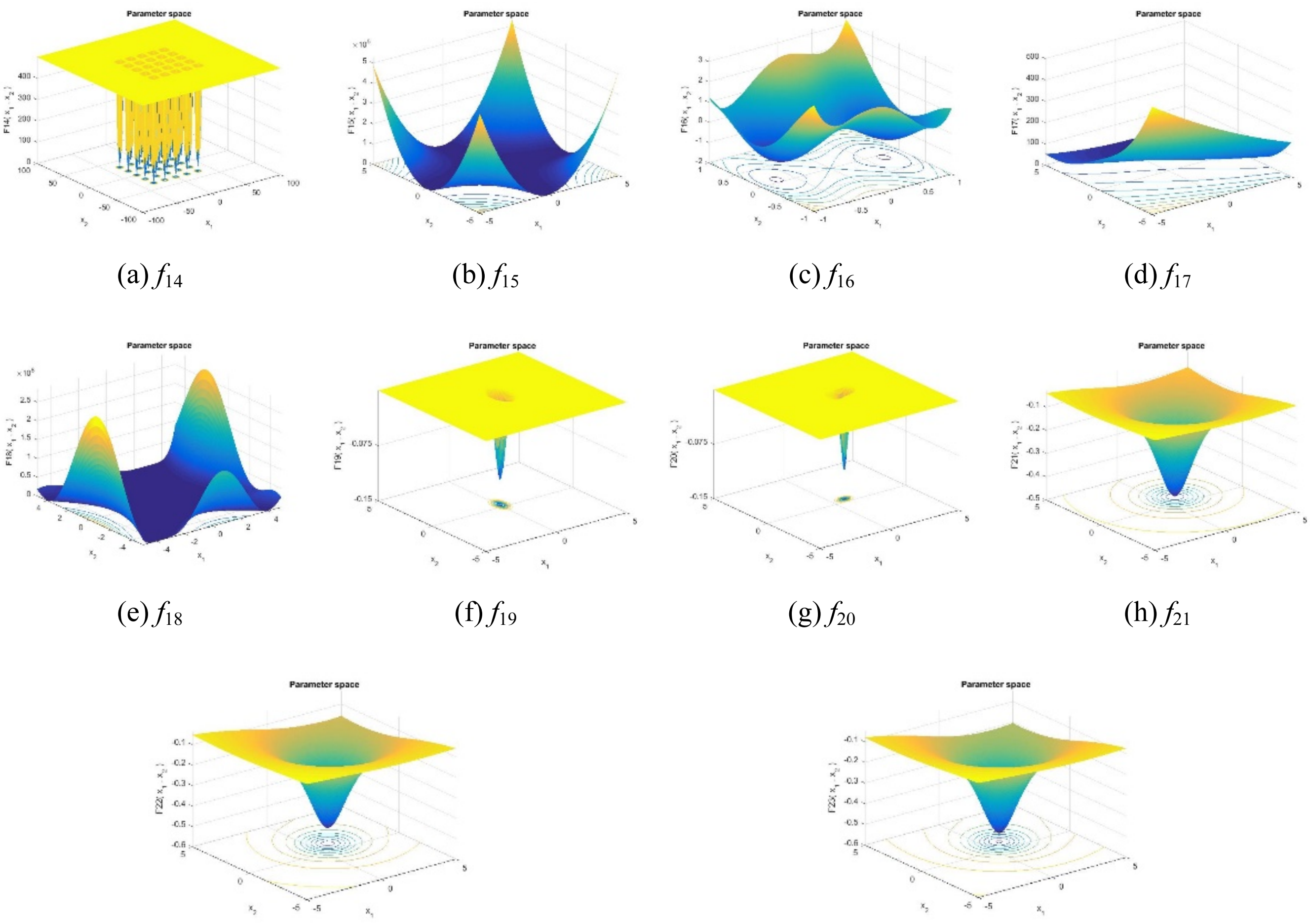

(a) f_{14} (b) f_{15} (c) f_{16} (d) f_{17}

(e) f_{18} (f) f_{19} (g) f_{20} (h) f_{21}

(i) f_{22} (j) f_{23}

Figure 8. 2-D Version of Fixed-Dimension Multimodal Benchmark Functions

Table 1. Parameter Setting

Algorithm	Parameter
PSO	$c = 2.0, w = 0.9, pop = 40, Iteration = 1000$
GBMO	$T = 900, a = 1.5, b = 1.2, pop = 40, Iteration = 1000$
PGBMO-DC	$T = 900, a = 1.5, b = 1.2, pop = 40, g = 4, Iteration = 1000$
PGBMO-EDC	$T = 900, a = 1.5, b = 1.2, pop = 40, g = 4, Iteration = 1000$
PGBMO-SRC	$T = 900, a = 1.5, b = 1.2, pop = 40, g = 4, Iteration = 1000$
PGBMO-DRC	$T = 900, a = 1.5, b = 1.2, pop = 40, g = 4, Iteration = 1000$

Table 2 shows the final results of each function, expressed as mean (AVG.) and standard deviation (STSD.). The top line of each function is the average (AVG.), and the bottom line is the standard deviation (STSD.). It can be seen from the column of GBMO that the superposition of italics and bold indicates that GBMO has better performance than PSO. It can be seen from the four parallel algorithms, namely PGBMO-DC (PG-DC), PGBMO-EDC (PG-EDC), PGBMO-SRC (PG-SRC) and PGBMO-DRC (PG-DRC), with better performance than GBMO is marked as bold. Finally, the comparison results of GBMO and PSO and the comparison results of four parallel algorithms and GBMO are calculated and marked in the table. If the comparison results of the two algorithms are similar, they are indicated by an underscore "----". In the comparison results, "WIN" represents the number of wins compared with the two algorithms. Similarly, "LOSE" and "SIMILAR" represent failure and similar results, respectively. This paper also marks the cases where the standard deviation (STSD.) winners of the two algorithms are marked as bold in similar cases. It is obvious from Table 2 that the four communication strategies proposed in this paper are far superior to the traditional GBMO algorithm.

Table 2. The Results of Simulation Experiments

Function	PSO		GBMO		PGBMO-DC		PGBMO-EDC		PGBMO-SRC		PGBMO-DRC	
	AVG.	STSD.	AVG.	STSD.	AVG.	STSD.	AVG.	STSD.	AVG.	STSD.	AVG.	STSD.
f1	2.26E+00	5.13E-01	**1.28E-02**	2.94E-04	**5.59E-06**	1.77E-10	**4.71E-04**	3.20E-06	**8.85E-04**	6.97E-06	**1.04E-04**	2.79E-08
f2	1.07E+00	2.03E-01	**3.03E-02**	4.98E-04	**1.52E-02**	2.19E-04	**1.86E-02**	4.45E-04	**6.88E-03**	5.64E-05	**1.80E-02**	3.19E-04
f3	1.54E+02	3.06E+03	**4.77E+01**	2.97E+04	**1.37E-01**	3.68E-02	**3.17E-01**	2.35E-01	**5.91E-01**	1.06E+00	**1.53E+00**	1.32E+01
f4	3.93E+00	4.15E+00	**8.00E-03**	9.30E-05	**2.93E-04**	6.73E-08	**1.31E-03**	6.85E-07	**2.48E-03**	6.92E-06	**2.91E-03**	2.19E-05
f5	1.89E+02	1.37E+04	**6.46E-04**	1.37E-06	**4.86E-04**	2.08E-06	4.71E-03	7.04E-05	**5.85E-05**	1.13E-08	4.17E-03	4.47E-05
f6	2.28E+00	4.84E-01	**1.10E-02**	2.67E-04	**4.60E-04**	3.20E-07	**7.80E-03**	1.84E-03	**5.95E-04**	7.48E-07	**1.07E-02**	2.19E-04
f7	1.33E-02	2.81E-05	**4.75E-04**	1.13E-07	**3.27E-04**	6.33E-08	**4.11E-04**	5.88E-05	**9.79E-05**	3.77E-09	5.11E-04	1.15E-07
f8	-6.17E+03	8.58E+05	**-1.16E+04**	2.77E+04	**-1.26E+04**	2.57E+02	**-1.25E+04**	1.63E+03	**-1.26E+04**	5.55E+00	**-1.25E+04**	2.25E+03
f9	2.93E+01	4.11E+01	**8.32E-03**	2.10E-04	**5.44E-04**	1.18E-06	**2.64E-03**	8.51E-06	**4.81E-04**	5.26E-07	**2.97E-03**	1.81E-05
f10	2.28E+00	1.57E-01	**7.20E-03**	5.54E-05	**2.19E-03**	3.07E-06	**3.70E-03**	1.05E-05	**2.57E-03**	6.05E-06	7.63E-03	2.43E-04
f11	1.00E+00	1.18E-03	**2.61E-03**	4.37E-06	**6.16E-04**	3.54E-06	**2.73E-04**	2.32E-07	**7.91E-04**	1.96E-06	**9.18E-04**	5.34E-06
f12	2.65E+00	2.89E+00	**2.06E-05**	1.11E-09	**1.88E-05**	8.00E-10	**1.45E-05**	4.09E-10	**2.35E-06**	2.38E-11	2.41E-04	1.60E-07
f13	3.06E-01	1.95E-02	**1.33E-05**	3.63E-10	**1.05E-05**	3.94E-11	1.72E-05	6.28E-10	**3.90E-06**	1.51E-11	3.51E-04	2.60E-06
f14	2.75E+00	2.70E+00	**9.98E-01**	1.89E-18	9.98E-01	**6.64E-20**	9.98E-01	**4.24E-17**	9.98E-01	**2.42E-20**	9.98E-01	4.85E-17
f15	6.06E-04	1.82E-07	1.66E-03	3.60E-09	**5.91E-04**	9.07E-08	**6.76E-04**	9.49E-08	**9.47E-04**	1.38E-07	**5.79E-04**	5.81E-08
f16	-1.03E+00	4.24E-16	-1.01E+00	3.72E-04	**-1.03E+00**	6.93E-11	**-1.03E+00**	8.20E-09	**-1.03E+00**	3.81E-07	**-1.03E+00**	6.15E-09
f17	3.98E-01	7.57E-15	4.18E-01	5.75E-04	**3.99E-01**	2.86E+00	**3.99E-01**	1.21E-06	**4.03E-01**	1.39E-05	**3.99E-01**	5.97E-07
f18	3.00E+00	1.24E-14	3.28E+00	7.89E-02	**3.01E+00**	5.68E-05	**3.09E+00**	1.02E-02	3.97E+00	3.59E-01	**3.07E+00**	4.67E-03
f19	-3.86E+00	4.09E-15	-3.73E+00	4.18E-03	**-3.85E+00**	3.47E-05	-3.36E+00	1.32E-01	-3.47E+00	6.63E-02	-3.34E+00	1.44E-01
f20	-3.27E+00	4.21E-03	-1.67E+00	2.21E-01	**-3.21E+00**	4.54E-02	-1.63E+00	2.65E-01	-1.64E+00	2.86E-01	**-1.72E+00**	2.06E-01
f21	-5.39E+00	9.31E+00	**-1.02E+01**	4.15E-07	-1.02E+01	**1.09E-08**	-1.02E+01	4.79E-07	-1.02E+01	3.70E-09	-1.02E+01	3.08E-06
f22	-6.82E+00	1.33E+01	**-1.04E+01**	1.05E-07	-1.04E+01	**1.87E-09**	-1.04E+01	8.40E-07	-1.04E+01	1.53E-08	-1.04E+01	3.39E-06
f23	-7.63E+00	1.46E+01	**-1.05E+01**	5.57E-07	-1.05E+01	**3.32E-09**	-1.05E+01	2.63E-06	-1.05E+01	2.12E-08	-1.05E+01	2.91E-06
WIN			17		19		15		16		13	
LOSE			6		0		4		3		6	
SIMILAR			0		4		4		4		4	

4.2 Unimodal Benchmark Functions

Unimodal functions are used most vividly by f1 to f6. They only have global optimal solutions. To verify the convergence speed of an algorithm, these 6 functions are usually used to implement it. Table 2 and Figure 9 show that the four optimization strategies proposed are far superior to PSO and GBMO. But in f5, PGBMO-EDC and PGBMO-DRC are in a slightly failed state compared to GBMO, and PGBMO-DRC is also relatively weak compared to GBMO. In most cases, these four parallel strategies not only converge fast but also quickly reach the global optimal. Therefore, if faced with a single-peak function, the algorithm proposed in this paper is very effective.

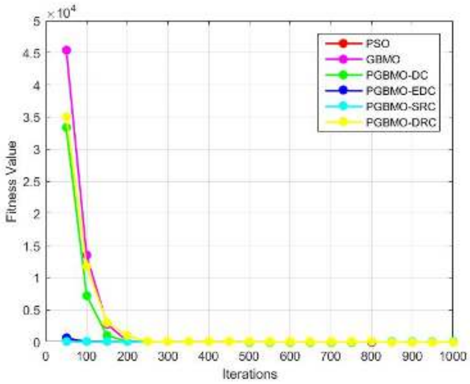

(a) f_1

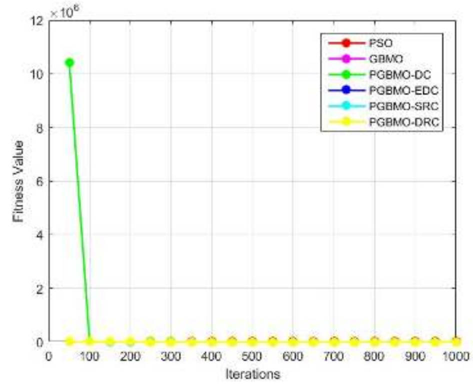

(b) f_2

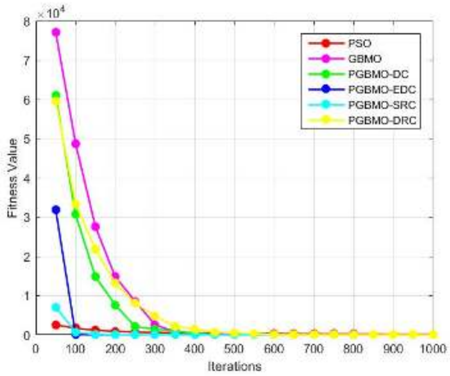

(c) f_3

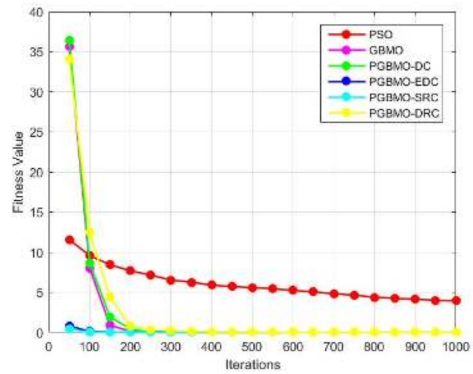

(d) f_4

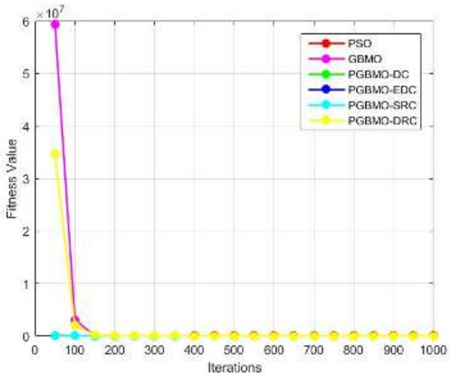

(e) f_5

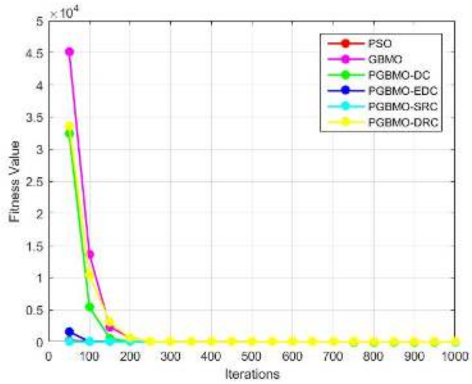

(f) f_6

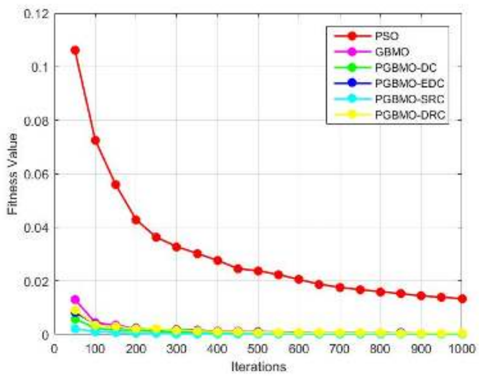

(g) f_7

Figure 9. Convergence Tendency for Unimodal Benchmark Functions

4.3 Multimodal Benchmark Functions

The f8-f13 is used to express Multimodal Functions well. Their characteristic is that there are so many difficulties to find the global optimal that it is almost difficult to find. Having many locally optimal solutions is a salient feature of these 9 functions. Table 2 and Figure 10 show that, although all algorithms are better than PSO, for some functions, their ability to avoid local optimization is still weak. In particular, PGBMO-DRC is particularly weak in such functions, which shows that it does not use the Multimodal Functions solution. The PGBMO-DC and PGBMO-SRC are excellent, which is conducive to their ability to give better solutions to such functions.

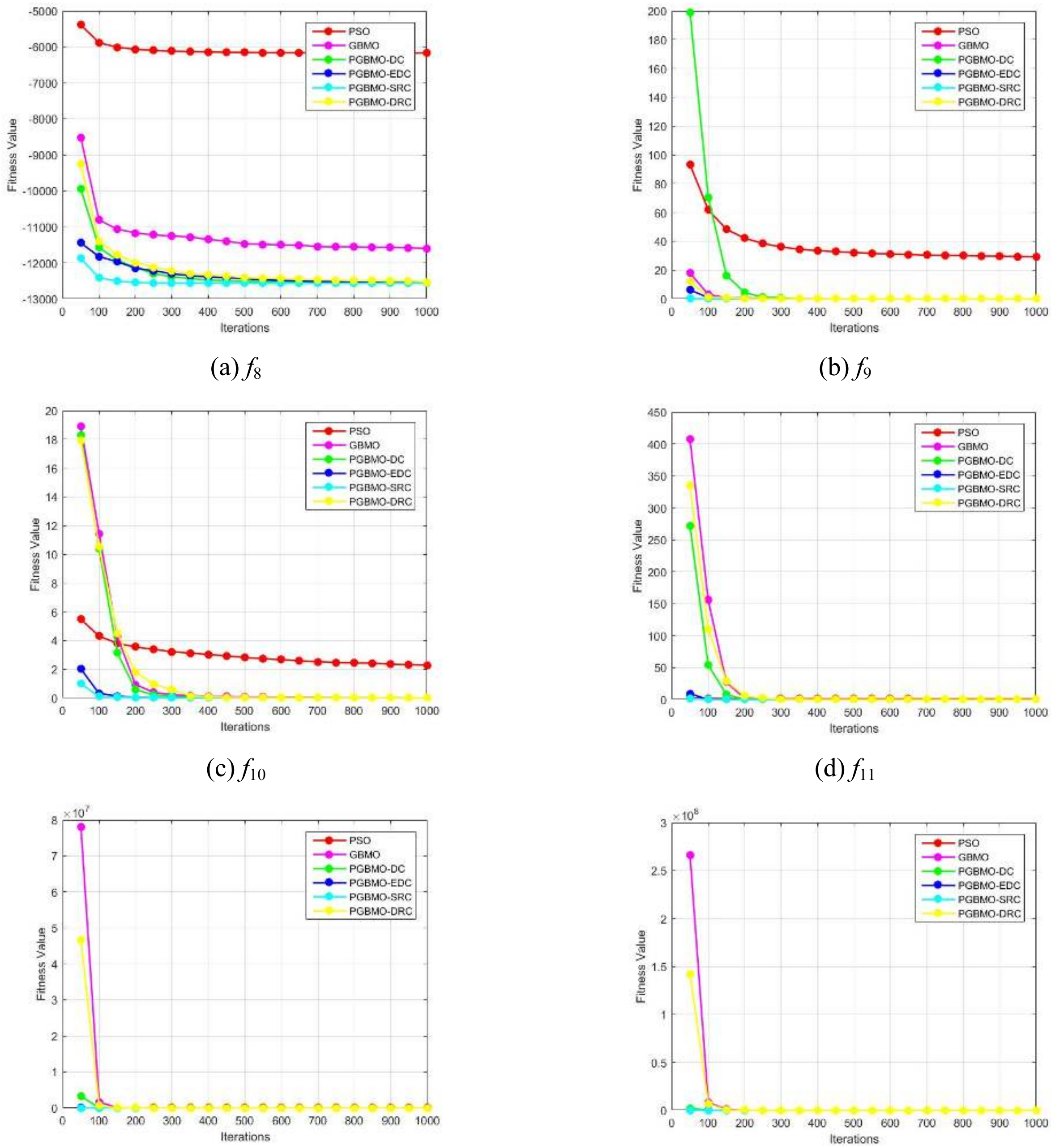

(a) f_8 (b) f_9

(c) f_{10} (d) f_{11}

(e) f_{12} (f) f_{13}

Figure 10. Convergence Tendency for Multimodal Benchmark Functions

4.4 Fixed-Dimension Multimodal Benchmark Functions

The f14-f23 is the performance of Fixed-Dimension Multimodal Functions. Their local optimal values are only a few, and the dimension is small. Table 2 and Figure 11 show that the PGBMO-EDC, PGBMO-SRC, and PGBMO-DRC algorithms proposed in this paper perform poorly in Fixed-Dimension Multimodal Functions, indicating that the algorithms we proposed are slightly unfavorable for solving such function problems. However, PGBMO-DC outperforms such functions. This shows that PGBMO-DC has the excellent convergence ability to avoid local optimization in solving such functions. And it can be seen that the four parallel methods proposed in this paper show good results in f21-f23, and quickly find the global optimal. This represents the advantages of the proposed algorithm.

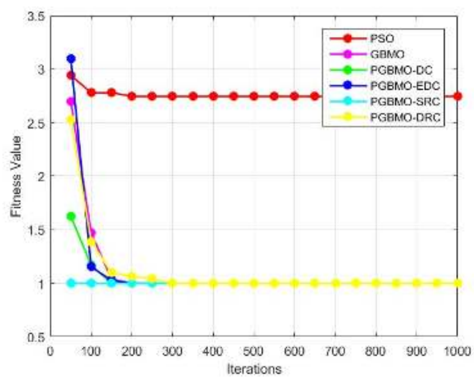

(a) f_{14}

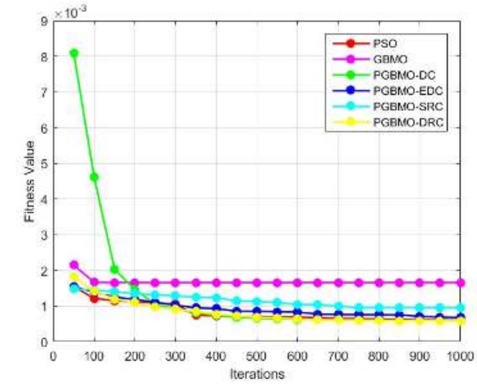

(b) f_{15}

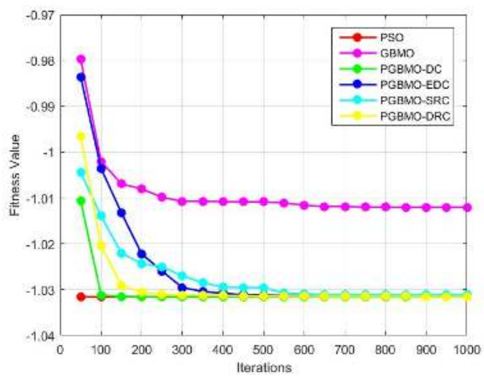

(c) f_{16}

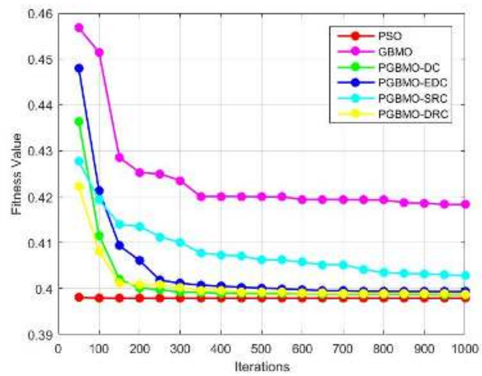

(d) f_{17}

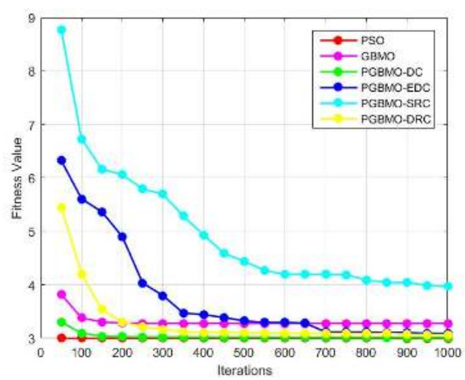

(e) f_{18}

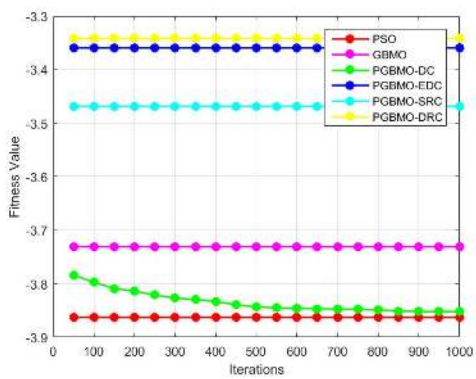

(f) f_{19}

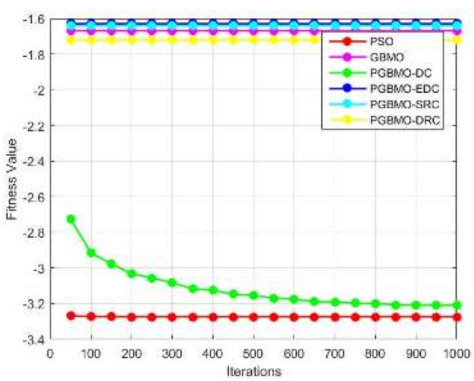

(g) f_{20}

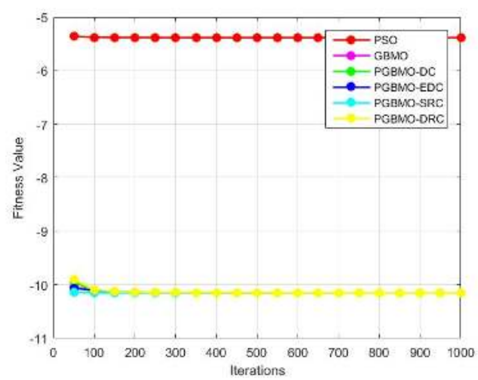

(h) f_{21}

Figure 11. Convergence Tendency for Fixed-Dimension Multimodal Benchmark Functions

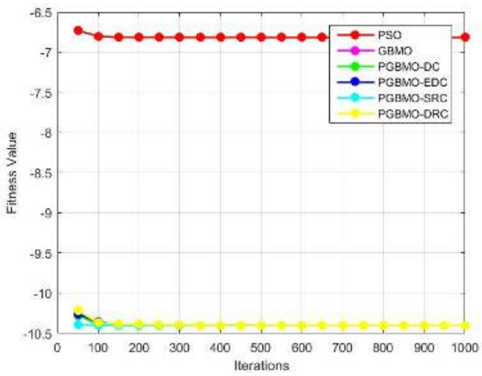

(i) f_{22}

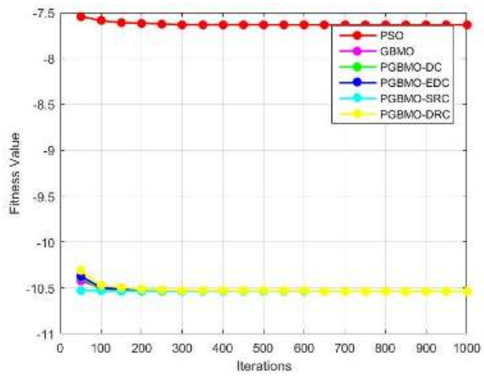

(j) f_{23}

Figure 11. Convergence Tendency for Fixed-Dimension Multimodal Benchmark Functions (continue)

5 WSN Coverage Optimization Experiment Simulation

5.1 Parameter Design

To test the effectiveness of the algorithm proposed in this paper for 3-D coverage of WSN, a simulation experiment is carried out on a plane with a terrain area of 50 × 50. The sensor nodes are randomly scattered in the three-dimensional terrain. The simulated 3-D terrain is shown in Figure 12. To fully verify the optimized performance of PGBMO on the coverage of WSN nodes, this article selects basic GBMO and traditional PSO and compares it. Use PSO and GBMO to apply to 3-D coverage, denoted as C-PSO and C-GBMO respectively. Use the parallel strategy mentioned in this article to optimize the three-dimensional coverage problem, which are denoted Coverage-PGBMO-DC (C-PGDC), Coverage-PGBMO-EDC (C-PGEDC), Coverage-PGBMO-SRC (C-PGSRC) and Coverage-PGBMO-DRC (C-PGDRC). The number of randomly deployed nodes varies from 30 to 80. The communication radius of the node ranges from [5m-30m]. The maximum number of iterations is set to 10. The number of populations is set to 20. For fair competition, each algorithm is simulated 30 times to take the average and standard deviation. The simulation parameters are shown in Table 3. Where the basic parameters of these algorithms are shown in Table 1. However, for every R_1 exchange of several parallel strategies, the parameters will be different, as shown in Table 3.

5.2 Sensor Node Incremental Mode Simulation

In order to effectively verify the performance of the algorithm proposed in this paper on three-dimensional coverage, this section uses sensor nodes to continuously change and other parameters unchanged for comparison. Table 4 records the coverage of sensor nodes [30-80] respectively. And record the average value of each algorithm to better compare its coverage.

Table 3. Experimental Settings for Parameters

Parameter Name	Parameter Values
Sensing region area	50m × 50m
population size	20
Number of iterations	10
Total number of sensor nodes	30-80
Communication range	5m-30m
C-PGDC	R_1 =5
C-PGEDC1	R_1 =5
C-PGEDC2	R_1 =2
C-PGSRC	R_1 =2
C-PGDRC	R_1 =2

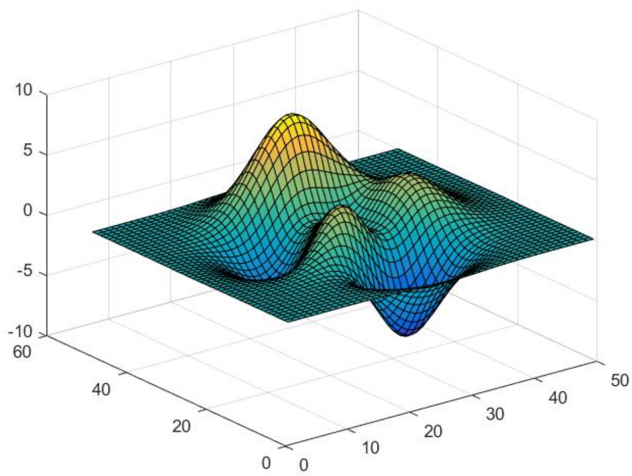

Figure 12. Topographic Map of Deployed Sensor Nodes

Table 4. Table of Sensor Nodes Increasing Network Coverage

Nodes Number	$Node_{30}$	$Node_{40}$	$Node_{50}$	$Node_{60}$	$Node_{70}$	$Node_{80}$	AVG.
C-PSO	0.4564	0.5504	0.6216	0.6913	0.7469	0.7854	0.6209
C-GBMO	0.4588	0.5554	0.6273	0.6912	0.7448	0.7853	0.6221
C-PGDC	0.4759	0.5660	0.6465	0.7056	0.7565	0.8013	0.6386
C-PGEDC1	0.4688	0.5646	0.6415	0.7028	0.7565	0.7990	0.6339
C-PGEDC2	0.4746	0.5664	0.6466	0.7070	0.7614	0.7995	0.6370
C-PGSRC	0.4684	0.5629	0.6403	0.7042	0.7535	0.7971	0.6328
C-PGDRC	0.4755	0.5740	0.6499	0.7127	0.7630	0.8057	0.6406

As can be seen from Table 4 and Figure 13, as the number of sensor nodes increases, the network coverage rate also continues to increase. Figure 13 shows that C-PGDRC coverage works best. Because C-PGDRC combines the advantages of PGDC's communication strategy and regrouping well, its coverage is the best in the field. It can also be seen from the Figure 14 that C-PGSRC is relatively weak, and it is relatively weak for solving the three-dimensional coverage problem. In short, it is obvious from Figure 14 that the strategy proposed in this paper is far superior to PSO and GBMO.

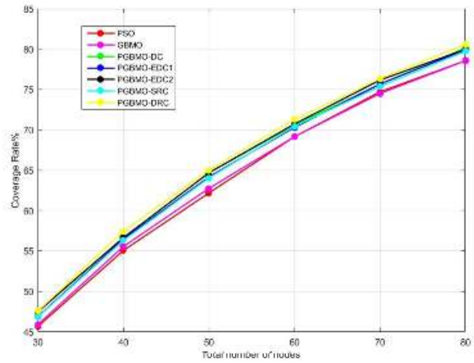

Figure 13. Graph of Increasing Network Coverage of Sensor Nodes

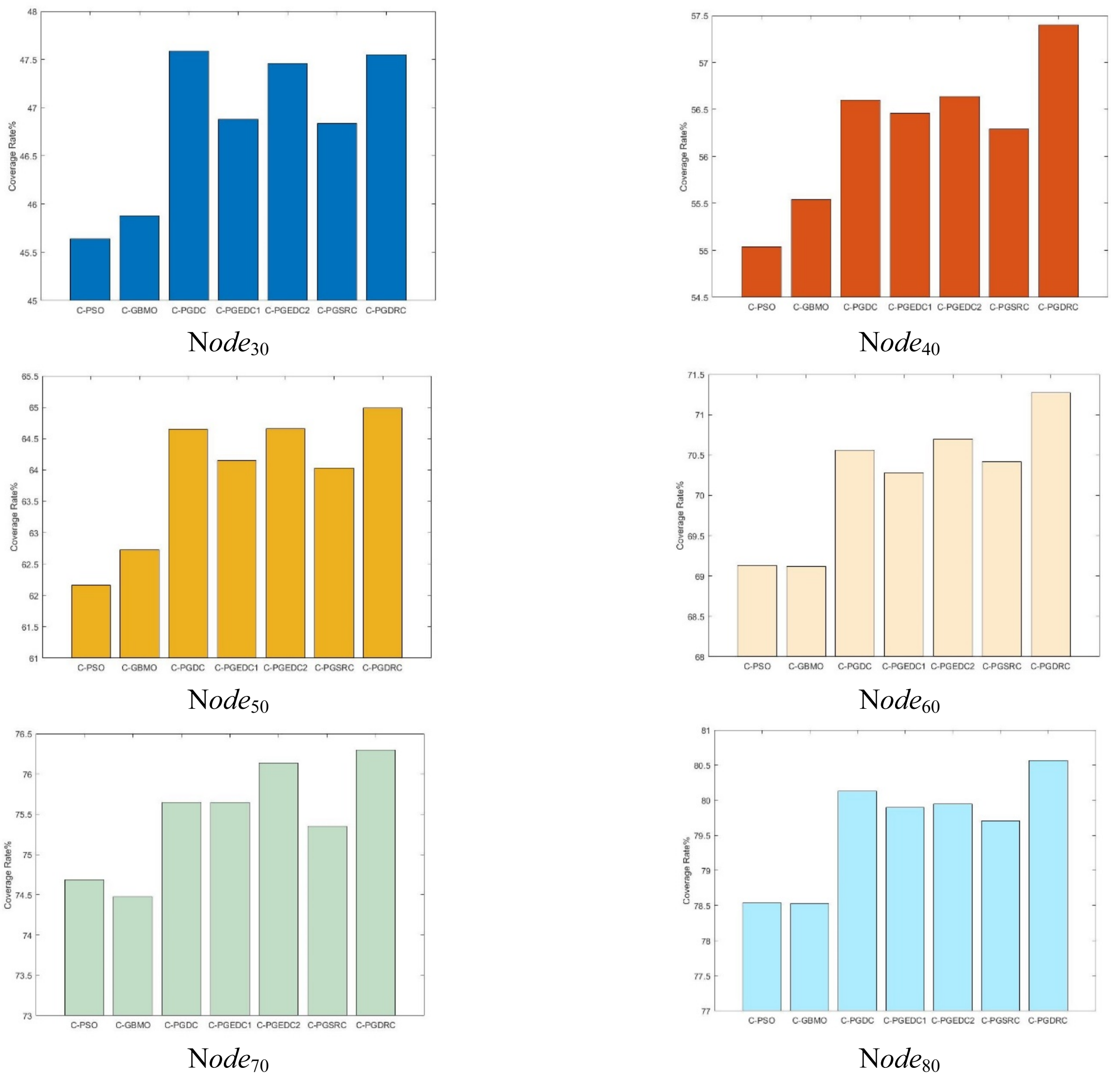

Figure 14. Histogram of Network Coverage with Varying Number of Nodes

5.3 Communication Radius Incremental Mode Simulation

Table 5 and Figure 15 show the coverage ratio with a communication radius of [5m-30m]. The results show that with the increase of the communication radius, the coverage gradually increases so that the coverage reaches 100% later. It can be seen from Table 5 that when the communication radius is large enough, the algorithm can achieve full coverage. To clearly see the significant change in coverage, Figure 16 plots the coverage of each algorithm. It can be seen from Figure 16 that when the communication radius is 15, the PSO and GBMO coverage has not yet been reached, and the parallel algorithm proposed in this paper achieves full coverage. This further proves the effectiveness of the proposed algorithm.

Table 5. Table of Communication Radius Increasing Network Coverage

Communication Radius	R_5	R_{10}	R_{15}	R_{20}	R_{25}	R_{30}	AVG.
C-PSO	0.4564	0.9397	0.9996	1	1	1	0.7282
C-GBMO	0.4588	0.9421	0.9998	1	1	1	0.7294
C-PGDC	0.4759	0.9568	1	1	1	1	0.7380
C-PGEDC1	0.4688	0.9514	1	1	1	1	0.7344
C-PGEDC2	0.4746	0.9596	1	1	1	1	0.7373
C-PGSRC	0.4684	0.9526	1	1	1	1	0.7342
C-PGDRC	0.4755	0.9638	1	1	1	1	0.7378

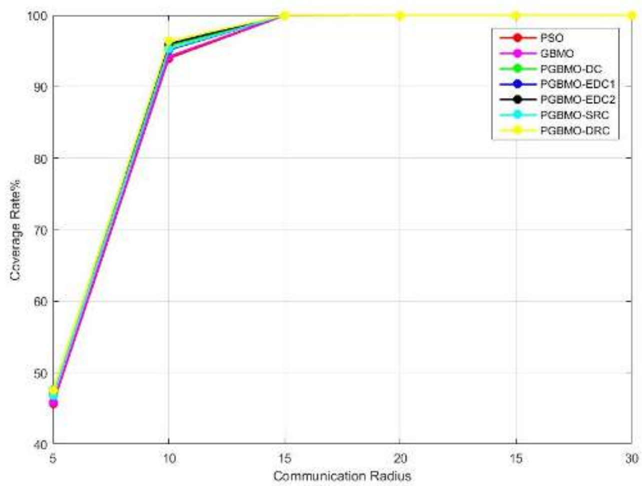

Figure 15. Graph of Increasing Network Coverage of Communication Radius

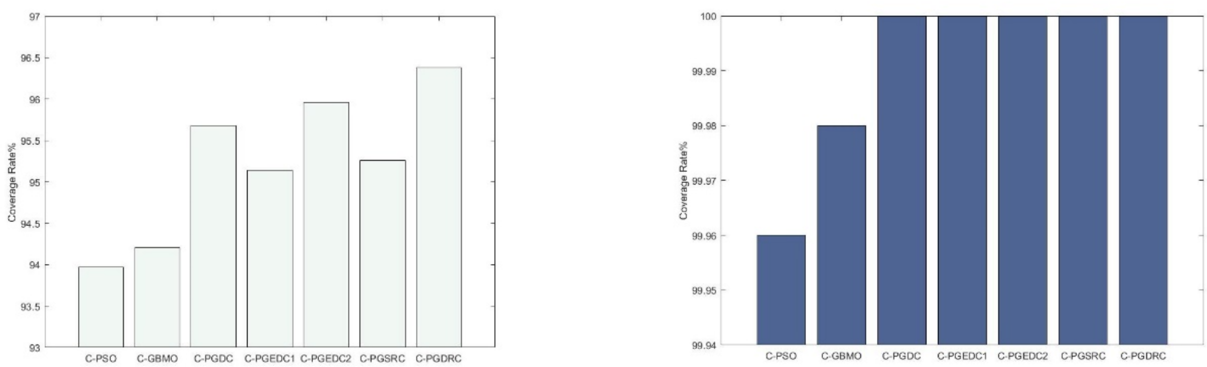

$Radius_{10}$ *$Radius_{15}$*

Figure 16. Histogram of Network Coverage with Varying Communication Radius

6 Conclusion

Efficient deployment of sensors to get maximum coverage plays an important role in WSN, in order to get the problems of 3-D coverage solved to improve the rate of coverage, this paper presented a modify GBMO algorithm that adopts four communication strategies to enhance the convergency, and took into consideration the concept of LOS to model WSN. Experiments on 23 benchmark functions composed of different types of functions proved that the efficiency of optimization convergency is well improved. Furthermore, the increase of coverage rate in WSN was demonstrated based on the random distribution of sensors and the changes of communication radius. In future research, we will further improve the problem of three dimensional coverage. The proposed methods may be further improved by applying some optimization methods [41-44].

References

[1] E. Sathiyamoorthy, K. Anusha, A decision tree-based rule formation with combined PSO-GA algorithm for intrusion detection system, *International Journal of Internet Technology and Secured Transactions*, Vol. 6, No. 3, pp. 186, January, 2016.

[2] S. C. Chu, X. Xue, J. S. Pan, X. Wu, Optimizing ontology alignment in vector space, *Journal of Internet Technology*, Vol. 21, No. 1, pp. 15-22, January, 2020.

[3] Q. Yang, S. C. Chu, J. S. Pan, C. M. Chen, Sine cosine algorithm with multigroup and multi-strategy for solving CVRP, *Mathematical Problems in Engineering*, Vol. 2020, pp. 1-10, March, 2020.

[4] A. Q. Tian, S. C. Chu, J. S. Pan, H. Cui, W. M. Zheng, A compact pigeon-inspired optimization for maximum short-term generation mode in cascade hydroelectric power station, *Sustainability*, Vol. 12, No. 3, pp. 767, February, 2020.

[5] C. Sun, Y. Jin, R. Cheng, J. Ding, J. Zeng, Surrogate-assisted cooperative swarm optimization of high-dimensional expensive problems, *IEEE Transactions on Evolutionary Computation*, Vol. 21, No. 4, pp. 644-660, August, 2017.

[6] W. Z. Guo, N. X. Xiong, C. Lee, L. T. Yang, G.-L. Chen, Q. Weng, Task Allocation Algorithm Based on Particle Swarm Optimization in Heterogeneous Computing Environments, *Journal of Internet Technology*, Vol. 11, No. 3, pp. 343-351, May, 2010.

[7] H. Wang, W. Wang, Z. Wu, Particle swarm optimization with adaptive mutation for multimodal optimization, *Applied Mathematics and Computation*, Vol. 221, pp. 296-305, September, 2013.

[8] J. S. Pan, P. C. Song, S. C. Chu, Y. J. Peng, Improved compact cuckoo search algorithm applied to location of drone logistics hub, *Mathematics*, Vol. 8, No. 3, pp. 333, March, 2020.

[9] T. G. Nguyen, C. So-In, G. N. Nguyen, Barrier Coverage Deployment Algorithms for Mobile Sensor Networks, *Journal of Internet Technology*, Vol. 18, No. 7, pp. 1689-1699, December, 2017.

[10] Z. G. Du, J. S. Pan, S. C. Chu, H. J. Luo, P. Hu, Quasi-affine transformation evolutionary algorithm with communication schemes for application of RSSI in wireless sensor networks, *IEEE Access*, Vol. 8, pp. 8583-8594, January, 2020.

[11] T. Y. Wu, C. M. Chen, K. H. Wang, C. Meng, E. K. Wang, A provably secure certificateless public key encryption with keyword search, *Journal of the Chinese Institute of Engineers*, Vol. 42, No. 1, pp. 20-28, January, 2019.

[12] T. Y. Wu, Z. Lee, M. S. Obaidat, S. Kumari, S. Kumar, C. M. Chen, An authenticated key exchange protocol for multi-server architecture in 5G networks, *IEEE Access*, Vol. 8, pp. 28096-28108, January, 2020.

[13] J. Wang, Y. Gao, K. Wang, A. K. Sangaiah, S. J. Lim, An affinity propagation-based self-adaptive clustering method for wireless sensor networks, *Sensors*, Vol. 19, No. 11, pp. 2579, June, 2019.

[14] Z. Qu, Y. Zhang, X. Peng, J. Li, K. Hu, An energy internet routing algorithm on hypergraph based minimum-energy loss, *Journal of Northeast Electric Power University*, Vol. 37, No. 6, pp. 93-99, December, 2017.

[15] C. H. Chen, C. A. Lee, C. C. Lo, Vehicle localization and velocity estimation based on mobile phone sensing, *IEEE Access*, Vol. 4, pp. 803-817, February, 2016.

[16] Z. Teng, Z. Qu, L. Zhang, S. Guo, Research on vehicle navigation BD/DR/MM integrated navigation positioning, *Journal of Northeast Electric Power University*, Vol. 37, No. 4, pp. 98-101, April, 2017.

[17] Y. F. Huang, C. H. Hsu, Energy efficiency of dynamically distributed clustering routing for naturally scattering wireless sensor networks, *Journal of Network Intelligence*, Vol. 3, No. 1, pp. 50-57, February, 2018.

[18] J. Li, X. Hou, Y. Wang, J. Huo, Quantum genetic uneven clustering algorithm for wireless sensor networks, *Journal of Information Hiding and Multimedia Signal Processing*, Vol. 9, No. 3, pp. 596-605, May, 2018.

[19] G. J. Horng, T. Y. Chang, The adaptive node selection mechanism scheme in solar-powered wireless sensor networks, *2014 International Conference on Intelligent Green Building and Smart Grid (IGBSG)*, Taipei, Taiwan, 2014, pp. 1-4.

[20] C. W. Tsai, P. W. Tsai, J. S. Pan, H. C. Chao, Metaheuristics for the deployment problem of WSN: A review, *Microprocessors and Microsystems*, Vol. 39, No. 8, pp. 1305-1317, November, 2015.

[21] J. S. Pan, C. Y. Lee, A. Sghaier, M. Zeghid, J. Xie, Novel systolization of subquadratic space complexity multipliers based on toeplitz matrix-vector product approach, *IEEE Transactions on Very Large Scale Integration (VLSI) Systems*, Vol. 27, No. 7, pp. 1614-1622, July, 2019.

[22] T. Adame, A. Bel, A. Carreras, J. Melia-Segui, M. Oliver, R. Pous, Cuidats: An RFID-WSN hybrid monitoring system for smart health care environments, *Future Generation Computer Systems*, Vol. 78, pp. 602-615, January, 2018.

[23] J. S. Pan, L. Kong, T. W. Sung, P. W. Tsai, V. Snášel, A clustering scheme for wireless sensor networks based on genetic algorithm and dominating set, *Journal of Internet Technology*, Vol. 19, No. 4, pp. 1111-1118, July, 2018.

[24] X. Fu, G. Fortino, W. Li, P. Pace, Y. Yang, WSNS-assisted opportunistic network for low-latency message forwarding in sparse settings, *Future Generation Computer Systems*, Vol. 91, pp. 223-237, February, 2019.

[25] M. Abdechiri, M. R. Meybodi, H. Bahrami, Gases brownian motion optimization: an algorithm for optimization (GBMO), *Applied Soft Computing*, Vol. 13, No. 5, pp. 2932-2946, May, 2013.

[26] C. Rathore, R. Roy, A novel modified gbmo algorithm based static transmission network expansion planning, *International Journal of Electrical Power & Energy Systems*, Vol. 62, pp. 519-531, November, 2014.

[27] S. Temel, N. Unaldi, O. Kaynak, On deployment of wireless sensors on 3-D terrains to maximize sensing coverage by utilizing cat swarm optimization with wavelet transform, *IEEE Transactions on Systems Man & Cybernetics Systems*, Vol. 44, No. 1, pp. 111-120, January, 2014.

[28] J. F. Chang, S. C. Chu, J. F. Roddick, J. S. Pan, A parallel particle swarm optimization algorithm with communication strategies, *Journal of Information Science and Engineering*, Vol. 21, No. 4, pp. 809-818, July, 2005.

[29] S. C. Chu, J. F. Roddick, J. S. Pan, Ant colony system with communication strategies, *Information Sciences*, Vol. 167, No. 1-4, pp. 63-76, December, 2004.

[30] J. S. Pan, P. Hu, S. C. Chu, Novel parallel heterogeneous meta-heuristic and its communication strategies for the prediction of wind power, *Processes*, Vol. 7, No. 11, pp. 845, November, 2019.

[31] X. Wang, J. S. Pan, S. C. Chu, A parallel multi-verse optimizer for application in multilevel image segmentation, *IEEE Access*, Vol. 8, pp. 32018-32030, February, 2020.

[32] Q. w. Chai, S. C. Chu, J. S. Pan, P. Hu, W. m. Zheng, A parallel WOA with two communication strategies applied in DV-Hop localization method, *EURASIP Journal on Wireless Communications and Networking*, Vol. 2020, No. 1, pp. 1-10, February, 2020.

[33] X. Sui, S. C. Chu, J. S. Pan, H. Luo, Parallel compact differential evolution for optimization applied to image segmentation, *Applied Sciences*, Vol. 10, No. 6, pp. 2195, March, 2020.

[34] J. Wang, C. Ju, Y. Gao, A. K. Sangaiah, G. j. Kim, A PSO based energy efficient coverage control algorithm for wireless sensor networks, *CMC-Computers, Materials & Continua*, Vol. 56, No. 3, pp. 433-446, January, 2018.

[35] J. S. Pan, L. Kong, T. W. Sung, P. W. Tsai, V. Snášel, α-fraction first strategy for hierarchical model in wireless sensor networks, *Journal of Internet Technology*, Vol. 19, No. 6, pp. 1717-1726, November, 2018.

[36] S. Mirjalili, S. M. Mirjalili, A. Lewis, Grey wolf optimizer, *Advances in engineering software*, Vol. 69, pp. 46-61, March, 2014.

[37] P. Hu, J. S. Pan, S. C. Chu, Improved binary grey wolf optimizer and its application for feature selection, *Knowledge-Based Systems*, Vol. 195, pp. 105746, May, 2020.

[38] F. Neri, E. Mininno, G. Iacca, Compact particle swarm optimization, *Information Sciences*, Vol. 239, pp. 96-121, August, 2013.

[39] N. Liu, J. S. Pan, T. T. Nguyen, A bi-population QUasi-Affine Transformation Evolution algorithm for global optimization and its application to dynamic deployment in wireless sensor networks, *Eurasip Journal on Wireless Communications & Networking*, Vol. 2019, No. 1, pp. 175, July, 2019.

[40] J. S. Pan, Q. W. Chai, S. C. Chu, N. Wu, 3-D Terrain Node Coverage of Wireless Sensor Network Using Enhanced Black Hole Algorithm, *Sensors*, Vol. 20, No. 8, pp. 2411, April, 2020.

[41] S. C. Chu, Z. G. Du, J. S. Pan, Symbiotic organism search algorithm with multi-group quantum-behavior communication scheme applied in wireless sensor networks, *Applied Sciences*, Vol. 10, No. 3, pp. 930, January, 2020.

[42] T. T. Nguyen, J. S. Pan, T. K. Dao, An improved flower pollination algorithm for optimizing layouts of nodes in wireless sensor network, *IEEE Access*, Vol. 7, pp. 75985-75998, June, 2019.

[43] J. S. Pan, N. Liu, S. C. Chu, A hybrid differential evolution algorithm and its application in unmanned combat aerial vehicle path planning, *IEEE Access*, Vol. 8, pp. 17691-17712, January, 2020.

[44] Z. Meng, J. S. Pan, K. K. Tseng, PaDE: An enhanced Differential Evolution algorithm with novel control parameter adaptation schemes for numerical optimization, *Knowledge-Based Systems*, Vol. 168, pp. 80-99, March, 2019.

Biographies

Min Gao received her B.S. degree from Nankai University Binhai College, China, in 2019. She is currently pursuing the master degree with the Northeast Electric Power University, Jinlin, China. Her research interests include intelligence algorithms and wireless sensor network.

Jeng-Shyang Pan received the B.S. degree in electronic engineering from the National Taiwan University of Science and Technology in 1986, the M.S. degree in communication engineering from National Chiao Tung University, Taiwan, in 1988, and the Ph.D. degree in electrical engineering from the University of Edinburgh, U.K., in 1996. He is currently the Director of the Fujian Provincial Key Lab of Big Data Mining and Applications, and an Assistant President with the Fujian University of Technology. He is also the Professor with the Harbin Institute of

Technology. He is the IET Fellow, U.K., and has been the Vice Chair of the IEEE Tainan Section. He was offered Thousand Talent Program in China in 2010.

Jian-po Li received his B.S., M.S., and Ph.D. from the Department of Communication Engineering, Jilin University, China, in 2002, 2005, and 2008, respectively. In 2008, he joined the School of Information Engineering, Northeast Electric Power University (NEEPU). He was a visiting scholar with New York University in 2013 and University of Ottawa in 2016. Now he is the full professor and Vice-dean of the School of Computer Science, NEEPU. His research interests focus on wireless sensor networks, intelligent signal processing, 5G, wireless power transmission.

Zi-pei Zhang, is a Junior student in the i-school Informatics major from the University of Washington. He will receive an M.S. degree in 2021 as graduated. He participated in the robotics team and also human-centered research groups in the college experience. He currently is studying Info classes about database and blockchain technology.

Qing-Wei Chai received the B.S. degree from the School of information management, Dezhou University, Dezhou, China, in 2018. He is currently pursuing the master's degree with the Shandong University of Science and Technology, Qingdao, China. His recent research interests include swarm intelligence and wireless sensor network.